

# The thermal expansion behaviour of highly oriented polyethylene

G. A. J. Orchard, G. R. Davies and I. M. Ward

Department of Physics, University of Leeds, Leeds LS 2 9JT, UK

(Received 17 October 1983; revised 13 January 1984)

The thermal expansion behaviour of oriented polyethylene has been studied over the temperature range  $-50^{\circ}\text{C}$  to  $+20^{\circ}\text{C}$ . In general the values for the thermal expansion coefficient in the orientation direction are negative and of a greater magnitude than the *c*-axis expansion for the crystal, which is approached at  $-50^{\circ}\text{C}$ . This remarkable effect has been quantitatively related to the influence of an internal shrinkage force, and the changes in expansivity with temperature shown to relate primarily to the change in modulus with temperature.

(Keywords: thermal expansion; shrinkage force; drawn polyethylene)

## INTRODUCTION

It has been recognized from recent research that there can be very large anisotropy in the linear thermal expansivities of oriented polymers<sup>1</sup>. There has been especial interest in the research for ultra high modulus polyethylene where it appeared that the expansivity parallel to the orientation direction ( $\alpha_{\parallel}$ ) was negative and apparently very close to the value ( $-12 \times 10^{-6} \text{ K}^{-1}$ ) for the *c*-axis expansion in the crystalline regions<sup>2,3</sup> obtained from X-ray measurements. This result was attributed to the high degree of crystal continuity in such highly oriented polymers and did not appear to be controversial. Recent work by Choy, Chen and Young<sup>4</sup>, however, has shown that in many polymers  $\alpha_{\parallel}$  can have a large negative value at high temperatures (as great as  $-10^{-4} \text{ K}^{-1}$ ). This was attributed to the contraction force exerted on the structure by taut tie-molecules. Due to the entropic nature of such forces, these increase in magnitude with increasing temperature and are therefore greatest at high temperatures.

These remarkable observations are of particular interest because they suggest that the thermal expansivity may be used as a probe to identify certain structural features in oriented polymers. We have therefore undertaken a thorough examination of the anisotropy of thermal expansivity in a range of highly drawn linear polyethylenes. A simple theoretical model is also proposed which provides a quantitative understanding of the temperature dependence of the linear expansivity. This model is very different from that proposed by Choy *et al.*, in that it suggests a connection between the expansivity  $\alpha_{\parallel}$ , the overall shrinkage force, and the temperature dependence of the modulus. Measurements have been made of the thermal expansion of samples of linear polyethylene (LPE) homopolymers and copolymers over a temperature range of  $-40^{\circ}\text{C}$  to  $20^{\circ}\text{C}$ . These have been supported by modulus measurements over the same range and by measurements of the shrinkage force obtained when the samples are immersed in an oil bath at the processing temperature.

Since the internal stresses incurred during processing depend on the method of preparation, samples have been drawn from three methods of production. These samples

occur as rods produced by hydrostatic extrusion or by die drawing and as films obtained by hot drawing isotropic sheets.

## EXPERIMENTAL

### Rod sample preparation

The hydrostatic extrusion of high density polyethylene has been described in detail in previous publications<sup>5,6</sup>. Essentially the present samples were produced as rods 2.5 mm diameter at deformation ratios of 5, 10, 15 and 20 and at an extrusion temperature  $100^{\circ}\text{C}$ . Two polymers were examined, a linear polyethylene homopolymer, Rigidex 006-60 and a methyl copolymer Rigidex 40. Details are given in Table 1.

The die drawing process through a heated conical die introduces a stress distribution different from that obtained with hydrostatic extrusion. Some of the deformation process occurs under non isothermal conditions beyond the die. Details of the procedure are reported elsewhere<sup>7</sup>. Current samples were produced from Rigidex 006-60 homopolymer and from Rigidex 002-55 butyl copolymer with a die temperature of  $100^{\circ}\text{C}$ . Polymer details are given in Table 1. Various draw ratios, with corresponding changes in diameter, were obtained by varying the draw speed.

Table 1 Details of the polymers

Polymer	$\bar{M}_n$	$\bar{M}_w$	Type	Process
Rigidex 50 (R50)	6 180	101 450	Homopolymer	Extruded rod at $100^{\circ}\text{C}$
R006-60	25 500	135 000	Homopolymer	Extruded rod at $100^{\circ}\text{C}$ Die drawn rod at $100^{\circ}\text{C}$ Drawn film at $75^{\circ}\text{C}$
R40	9 600	93 600	Methyl copolymer	Extruded rod at $100^{\circ}\text{C}$
R002-55	19 400	167 500	Butyl copolymer	Die drawn rod at $100^{\circ}\text{C}$ Drawn film at $75^{\circ}\text{C}$

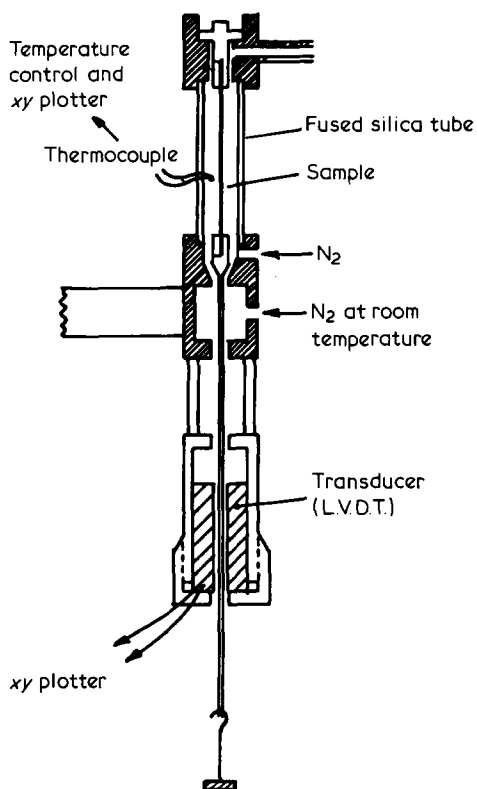


Figure 1 Schematic diagram of the thermal expansion apparatus for film strip measurements

**Film sample preparation**

Isotropic sheets approximately 0.5 mm thick of Rigidex 006-60 homopolymer and of Rigidex 002-55 butyl copolymer were obtained by compression moulding at 160°C followed by quenching into water at 20°C. Dumbbell

samples with gauge dimensions 20 × 2 mm were cut from these sheets and drawn in air at 75°C on an Instron tensile testing machine at a crosshead speed of 10 cm/min. The drawing times for various samples were varied to obtain draw ratios of about 5, 10, 15 and 20 as determined by the displacement of ink marks on the surface originally made at 1 mm intervals on that of the undrawn sample.

**Thermal expansion**

Thermal expansion measurements were made on equipment developed in the laboratory. The film measurement equipment is illustrated schematically in Figure 1. The samples about 6 cm long are suspended inside a fused silica tube in a stream of nitrogen gas whose temperature can be controlled. A clamp attached to the lower end of the sample is attached to a rod carrying the slug of a LVDT transducer. The rod passes through the centre of the transducer and provision is made for adding weights. To reduce instrumental expansion effects, the upper and intermediate parts of the equipment are constructed in Invar and both the inner clamps and the outer casing are of similar lengths. The lower cylinder containing the transducer coils is made of stainless steel and is separated from the other units by three stainless steel rods to reduce heat transfer between the sample enclosure and the transducer. As a further precaution a slow flow of nitrogen at about room temperature is passed through the lower chamber of the intermediate section.

The temperature of the nitrogen flowing past the sample is determined by a copper constantan thermocouple located near the centre of the sample. By interposing suitable millivolt levels in the thermocouple loop the balance position of the temperature controller can be adjusted to obtain different temperatures. The thermocouple output provides the X-deflection on an XY

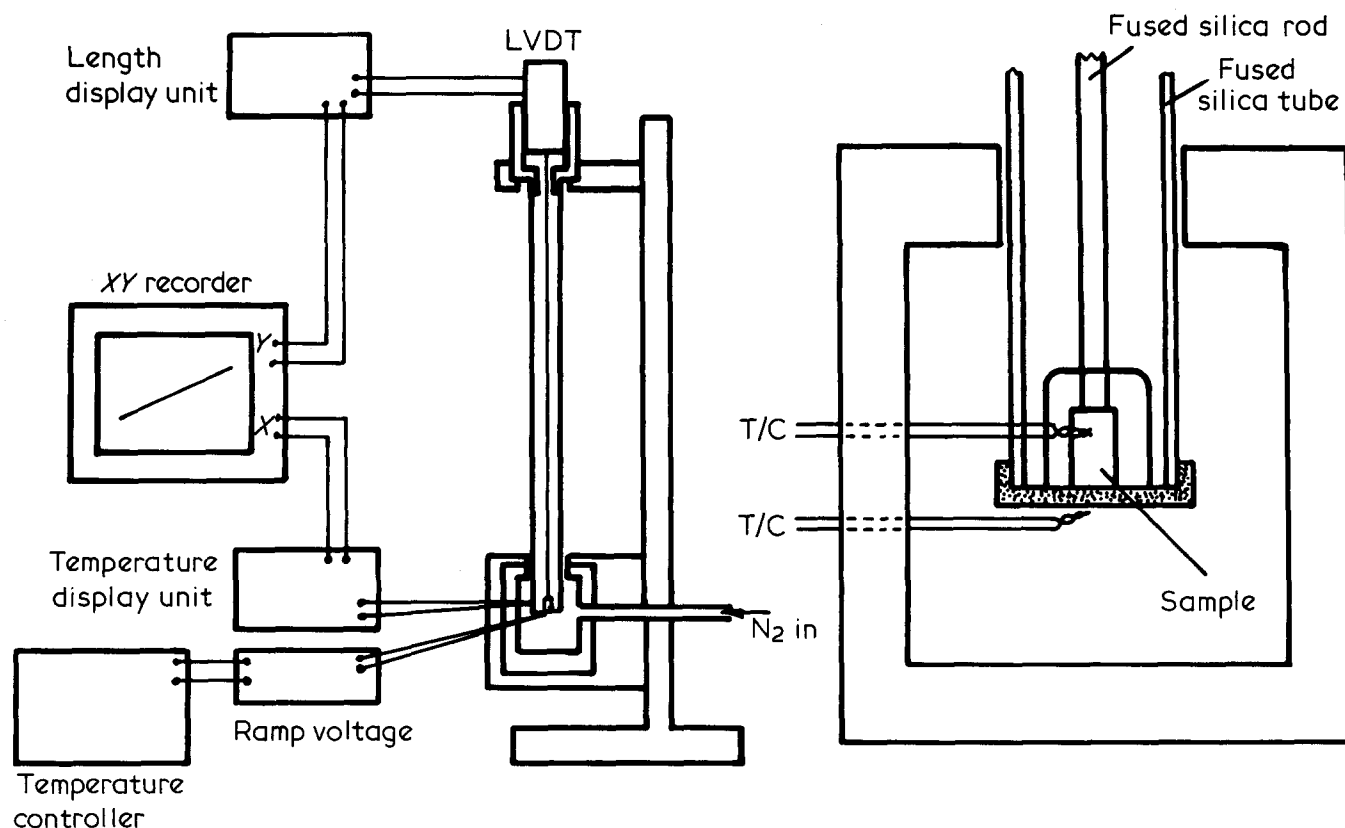


Figure 2 Schematic diagram of the thermal expansion apparatus for rod measurements

**Table 2** Values derived from the film measurements for the stress constant  $B$  and the intrinsic expansion coefficient  $\alpha_0$  in equation (6) with calculated internal stresses at the processing temperature and measured shrinkage stresses

Polymer	Draw ratio	$\alpha_0 \times 10^6$	$B$ (MPa/°C)	Calculated stress at 76°C (MPa)	Measured shrinkage stress at 76°C (MPa)
R006-60	11	-11.9	0.033	12	18
	20	-9.3	0.075	26	24
R002-55	5.5	-12.7	0.019	6.5	14
	11	-12.1	0.048	17	29
	19	-10.3	0.074	26	31

plotter while the Y deflection is obtained from the LVDT transducer.

Measurements were made by abrupt changes in the millivolt level between upper and lower limits corresponding to about 10°C interval changes. The corresponding position changes on the XY plotter then provided  $dl/dT$  from which the expansion coefficient could be calculated. The small thermal capacity of the film strips provided a rapid temperature response so that the change in position on the recorder could be achieved within 1 minute and positions were checked by 2 or 3 runs in each direction. Check measurements were also made with copper wires. Repeat measurements and the wire results indicate an accuracy of  $\pm 0.6 \times 10^{-6}$  in the expansion coefficients.

For the rod measurements a similar transducer was used but with samples about 6 millimetres long under slight compression. The apparatus is shown schematically in Figure 2. The samples are supported by an Invar platform cemented to the lower end of a fused silica tube. A cut out at the bottom of the tube provides access for samples and ventilation. The upper end of the fused silica is attached to an Invar cylinder providing a housing for the outer casing of the length sensing transducer (LVDT). On the top of the sample rests a fused silica rod which passes down the centre of the silica tube and is attached at its upper end to an Invar rod carrying the slug of the transducer. Contact is maintained by slight spring pressure giving a load of 35 g on the sample. The lengths of the silica rod and tube are approximately equal to avoid any differential thermal expansion effects. The bottom 3 cm of the tube are contained within an insulated controlled temperature enclosure. With this form of construction and an 18 cm tube length the transducer is sufficiently separated from the enclosure to avoid spurious temperature effects during measurements.

As before, temperature control is achieved with a continuous flow of nitrogen gas through the enclosure with copper-constantan thermocouples as sensors. One thermocouple is placed in the gas stream immediately below the Invar base plate to control the temperature of the incoming gas while a second is located close to the sample within the silica tube. The temperature and length changes again provide the X and Y deflections respectively on an XY plotter but the temperature change is carried out more slowly, at about  $1\frac{1}{2}$ °C per min, to allow the sample and equipment to reach equilibrium. Ranges covered were -10°C to 15°C and -55°C to -25°C. A small instrumental correction was determined by measurements on a fused silica sample. Repeat

measurements indicate an accuracy of  $\pm 0.6 \times 10^{-6}$  for  $\alpha_{||}$  values and  $\pm 2\%$  for the larger  $\alpha_{\perp}$  values.

#### Modulus measurements

The thermal expansion measurements necessarily require a comparatively long time scale to reach equilibrium conditions. This is particularly the case for the rod measurements. The modulus relevant to any change in stress with temperature is consequently a creep modulus rather than a dynamic modulus.

For the films the samples were suspended in a constant temperature enclosure and measurements made of the 10 s extensional modulus. Both the modulus and the expansion observations were made on the same samples.

The same technique was not possible for the small rod samples and hence, for these, longer samples were used (~15 cm) and the modulus determined from a three point bend test. In this test the sample is supported horizontally at two points and a load is applied at the centre. In this case, in view of the longer expansion measurement period, the deflection obtained 1 min after application of the load was observed, to derive an equivalent 1 min modulus. Details of the method have been reported elsewhere<sup>8</sup>. Measurements were made at various temperatures with the sample and supports in a temperature controlled enclosure.

#### Shrinkage force measurements

The shrinkage and shrinkage force generated when drawn samples are heated have been the subject of earlier investigations into the structure of ultra high modulus polyethylenes<sup>9</sup>. The shrinkage force measurements of the films were made by clamping 8 cm lengths in a framework, one end of which was linked through a pivot to a resistance strain gauge transducer. The output from the transducer was fed to a chart recorder to observe the variation in the shrinkage force with time when the sample was immersed in a silicone oil bath at a constant elevated temperature. A bath temperature of ~76°C was used corresponding to the temperature of drawing. At this temperature the shrinkage force slowly develops with time to a maximum and the values thus obtained are shown in Table 2. Details of the equipment are given in the reference.

The forces involved in similar measurements on the rods are much greater and are outside the range of the film equipment. Measurements have therefore been confined to a modified form of the apparatus (Figure 3) attached to an Instron Tensile Tester where the sample is fixed and the silicone oil level is raised to immerse the specimen.

## RESULTS

A number of measurements on the rod samples were carried out over two temperature ranges, namely -10°C to +15°C and -30°C to -50°C. The variation of the expansion coefficients within these ranges was sufficiently small for a straight line to be drawn to obtain the slope,  $dl/dT$ , of the resulting XY plots and hence the expansion coefficient  $(1/l)(dl/dT)$ . The thermal expansion coefficients obtained in this way with the extruded rods in the higher temperature range, -10°C to +15°C, are shown in Figure 4 with some repeat measurements carried out on some Rigidex 50 samples obtained from earlier studies. As can be seen in Rigidex 50 values obtained for  $\alpha_{||}$ , the

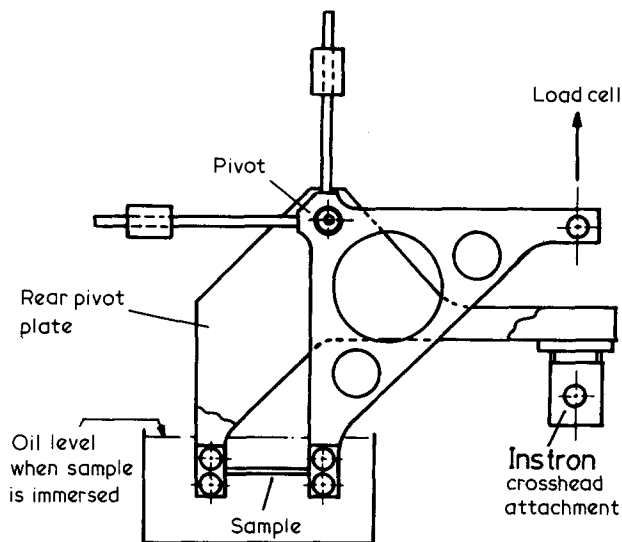


Figure 3 Schematic diagram of the Instron attachment to measure shrinkage force on rod samples. Front pivot plate has been removed to show the load cell 'moving' plate

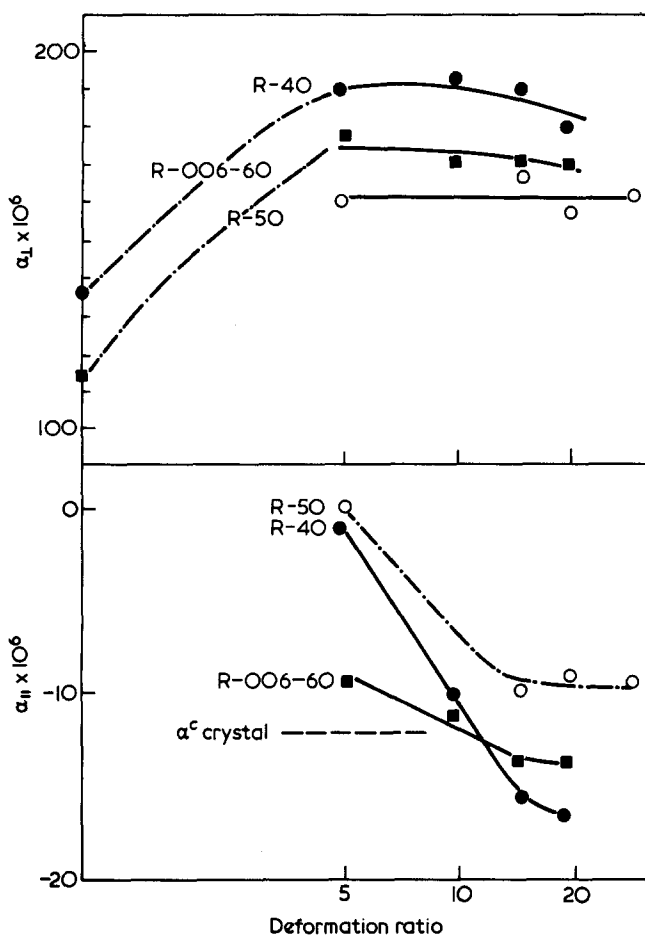


Figure 4 Variation of the thermal expansion coefficients for the temperature range  $-10^{\circ}\text{C}$  to  $+15^{\circ}\text{C}$  with deformation ratio for extruded polyethylene

coefficient in the axial direction, decreases with deformation ratio but do not fall beyond the value of  $-12 \times 10^{-6} \text{ K}^{-1}$  obtained for the  $c$ -axis expansion in the crystal found by X-ray measurements. On the other hand the coefficients of 006-60 samples are below the crystal value for the two higher deformation ratios and those for the Rigidex 40 copolymer are even lower.

Repeat measurements of the axial expansion coefficient in the lower temperature range,  $-30^{\circ}\text{C}$  to  $-50^{\circ}\text{C}$ , are

shown in Figure 5 and these show a general increase in all the values. Even the Rigidex 40 copolymer approaches the polyethylene  $c$ -axis crystal value.

A similar pattern is obtained with the die drawn results shown in Figures 6 and 7. The 002-55 copolymer axial expansion coefficient is below  $-18 \times 10^{-6}$  in the higher temperature range but is only just below the crystal value in the region of  $-40^{\circ}\text{C}$  as can be seen in Table 3.

Measurements on the films were made with a narrower temperature range but at various mean temperatures between  $-40^{\circ}\text{C}$  and  $+20^{\circ}\text{C}$ . Both the 006-60 homopolymer and the 002-55 copolymer results, plotted against temperature in Figures 8 and 9 respectively, show a much greater range of expansion coefficients than was obtained with the rods. Moreover the values obtained for the lower draw ratios are now below those of the higher draw ratios. The variation with draw ratio is shown in Figure 10 for the two polymers at two temperature levels. As with the rods, the copolymer shows lower expansion coefficients than the corresponding homopolymer at the same draw ratio. At the lower temperature the coefficients for the highest draw ratio are again close to the crystal  $c$ -axis value.

### DISCUSSION

In an article primarily concerned with the effects of orientation in amorphous polymers, Struick<sup>10</sup> considered the effects of internal stress. He observed that in amorphous polymers the thermal expansivity  $\alpha_{||}$  falls with increasing orientation, and attributed this to the increasing effect of an entropic internal stress with increasing orientation. He also noted that similar results had been observed for crystalline polymers, and concluded that the negative expansion coefficients observed were not due to their crystalline nature but to the frozen in entropic stress. No attempt was made to quantify the effects of internal stress, nor was there any explicit consideration of the change in expansion coefficients with temperature.

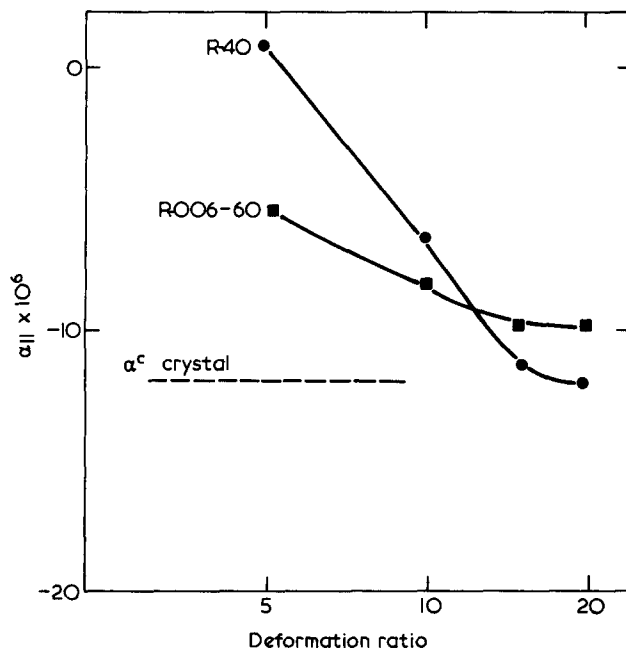
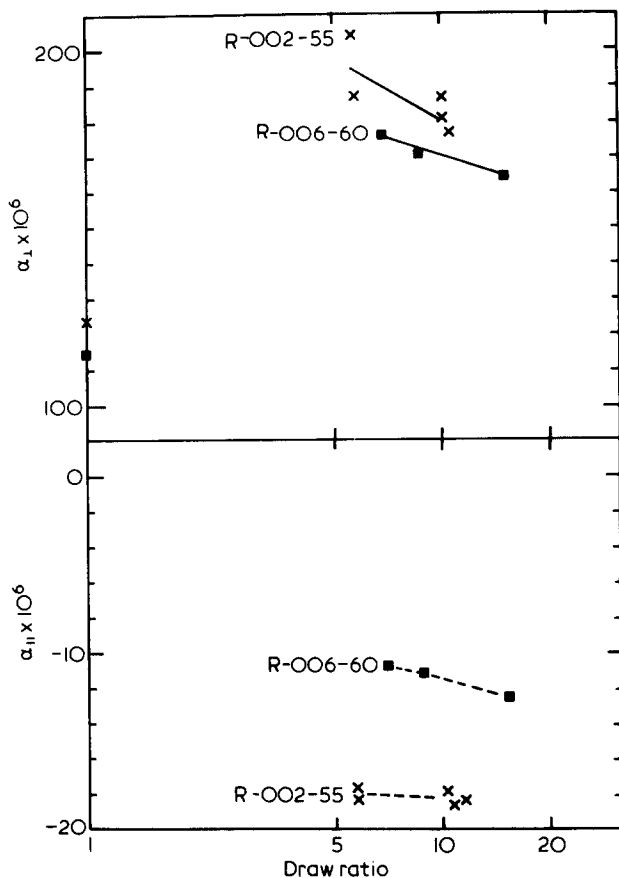
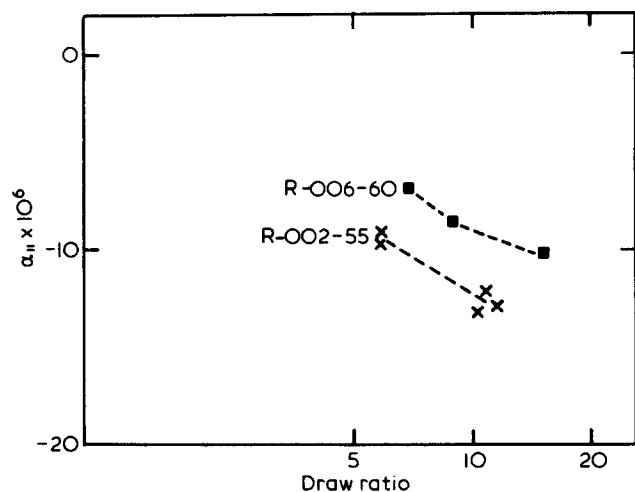


Figure 5 Variation of the axial thermal expansion coefficient for the temperature range  $-30^{\circ}\text{C}$  to  $-50^{\circ}\text{C}$  with deformation ratio for extruded polyethylene rod samples



**Figure 6** Variation of the thermal expansion coefficients for the temperature range  $-10^{\circ}\text{C}$  to  $+15^{\circ}\text{C}$  with draw ratio for die drawn polyethylene rod samples



**Figure 7** Variation of the axial thermal expansion coefficient for the temperature range  $-30^{\circ}\text{C}$  to  $-50^{\circ}\text{C}$  with draw ratio for die drawn polyethylene rod samples

In a comprehensive survey of the thermal expansion behaviour of crystalline polymers, Choy, Chen and Young<sup>4</sup> observed that in several oriented polymers  $\alpha_{\parallel}$  is negative at high temperatures. Oriented low density polyethylene, for example, shows values in the region of  $-2 \times 10^{-4} \text{ K}^{-1}$  at room temperature. It was suggested that this was due to the rubber-like forces of contraction of taut-tie molecules between the crystal blocks. For polymers of high crystallinity it was noted that  $\alpha_{\parallel}$  appeared to reach a value near  $\alpha_{\parallel}^c$ , the thermal expansivity of the crystalline regions. This was attributed to the constraining effect of the crystal bridges. The model proposed by Choy *et al.* is shown in Figure 11. It can be

seen that the taut-tie molecules are in parallel with the crystal bridges and the remaining amorphous material, and that all three are in series with the main bulk of crystalline material.

This model provides a quantitative prediction for the thermal expansivity  $\alpha_{\parallel}$ . Essentially the equation for  $\alpha_{\parallel}$  is

**Table 3** Thermal expansion coefficients for die-drawn rod samples in two temperature ranges

Polymer	Draw ratio	Temperature range $-10^{\circ}\text{C}$ to $+15^{\circ}\text{C}$		Temperature range $-30^{\circ}\text{C}$ to $-50^{\circ}\text{C}$
		$\alpha_{\parallel} \times 10^6$	$\alpha_{\perp} \times 10^6$	$\alpha_{\parallel} \times 10^6$
R006-60	6.9	-10.4	176	-7.0
	8.8	-10.8	171	-8.6
	15.4	-12.1	164	-10.3
R002-55	5.7	-18.2	204	-9.5
	5.8	-17.8	187	-9.1
	10.3	-17.8	181	-13.3
	10.7	-18.6	177	-12.2
	11.5	-18.5	187	-12.9

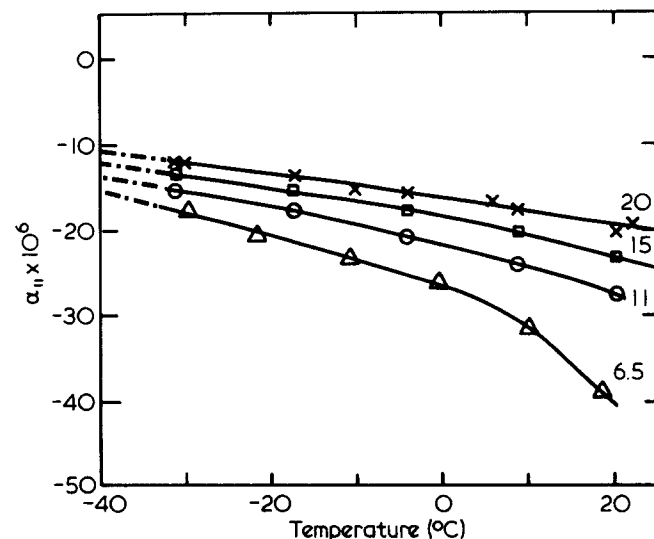


**Figure 8** Variation of the longitudinal thermal expansion coefficient of drawn 006-60 homopolymer polyethylene film strip with temperature. Numbers by the curves indicate the draw ratio

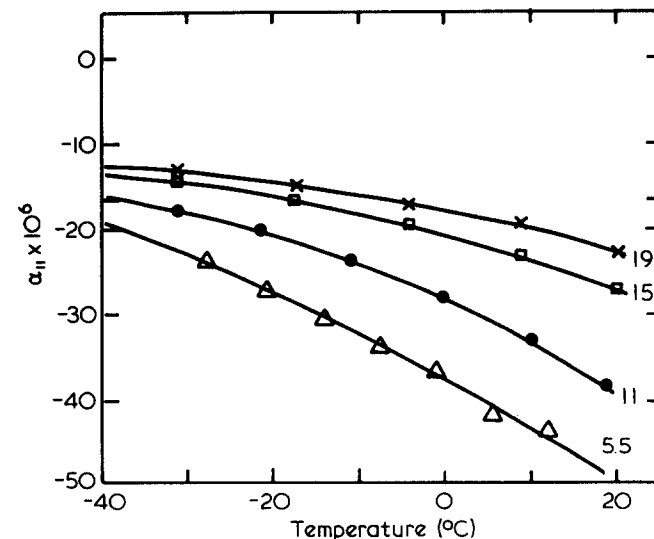


**Figure 9** Variation of the longitudinal thermal expansion coefficient of drawn 002-55 copolymer polyethylene film strip with temperature. Numbers by the curves indicate the draw ratio

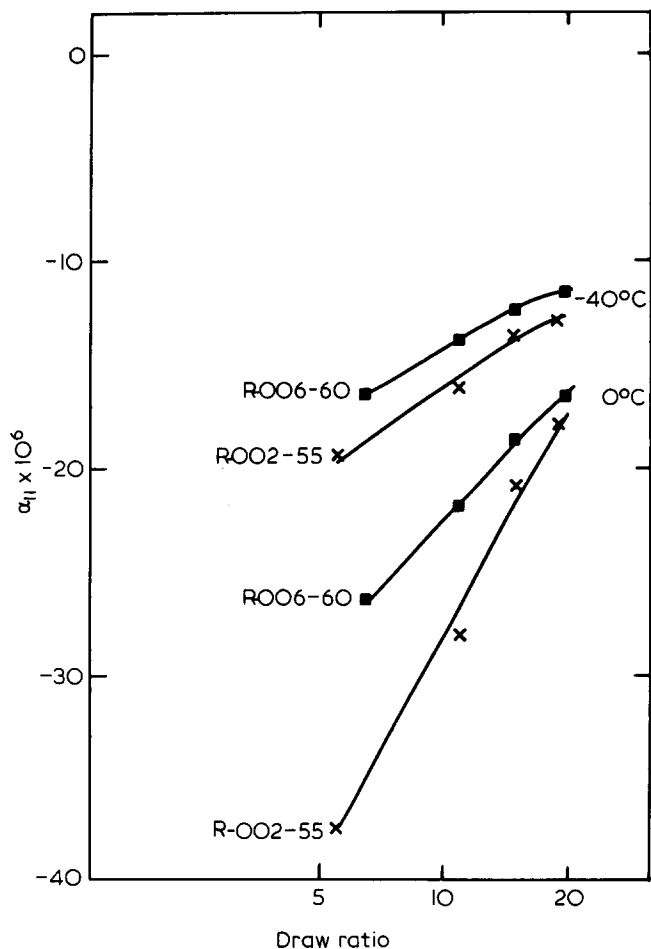


Figure 10 Variation with draw ratio at two different temperatures of the thermal expansion coefficients for the drawn films

given by 
$$\alpha_{\parallel} = \alpha_0 - (1 - y) \frac{1}{T} \frac{tE^t}{bE_{\parallel}^c} \quad (1)$$

where  $y$  = crystalline block volume fraction;  $b, t$  are the volume fractions of remaining material of bridge and taut-tie molecules respectively;  $E^t$  is the modulus of the tie molecules; and  $E_{\parallel}^c$  is the modulus of the crystalline material (i.e. crystal bridges and crystal block).

If we disregard the small contribution from the amorphous component the modulus of the polymer is given by

$$\frac{1}{E} = \frac{y}{E_{\parallel}^c} + \frac{1-y}{bE_{\parallel}^c + tE^t} \quad (2)$$

For low density polyethylene Choy *et al.* show that the values of  $\alpha_{\parallel}$  and  $E$  at 320 K are consistent with  $b \approx 10^{-3}$ ,  $t \approx 10^{-1}$  and  $E^t \approx 0.75$  GPa. It is of particular interest to note the very small proportion of crystal bridges, and the comparatively high value of  $E^t$ . For linear polyethylene this treatment was also applied to  $\alpha_{\parallel}$  at 320 K and using a value for  $b$  of  $4 \times 10^{-2}$  obtained by X-ray measurements,  $t$  was about  $2 \times 10^{-2}$ .

This analysis has a number of interesting implications. First the internal stresses due to the tie molecules are quite large, certainly much larger than the observed shrinkage stresses in LPE, which have been shown to lie in the range 10–30 MPa. Secondly, the taut-tie molecules contribute substantially to the modulus. Finally combining equations (1) and (2) we have

$$\alpha_{\parallel} - \alpha_0 = -(1 - y) \frac{1}{T} \times \left[ \left( \frac{1-y}{b} \right) \left( \frac{E}{E_{\parallel}^c - yE} \right) - 1 \right] \quad (3)$$

The r.h.s. of equation (3) essentially decreases in magnitude with increasing temperature i.e.  $\alpha_{\parallel} - \alpha_0$  is predicted to become closer to zero as temperature increases, which is contrary to observations.

We will now propose an alternative model, which is in the spirit of the ideas proposed by Struick, but attempts to quantify the situation. It is necessary to decide explicitly the connectivity relationships between the stiffness and the internal stress. We imagine the structure to consist of two components acting mechanically in parallel. The first component is responsible for the stiffness of the sample and may consist of lamellae, intercrystalline bridges, taut-tie molecules, etc. The second component, which provides an internal stress, is seen as a large scale network which intermingles with the first component. This network is assumed to make an insignificant contribution to the modulus but provides the retractive stress measured in a macroscopic shrinkage force experiment. Whereas the sample moduli are in the range 10–50 GPa, rubber moduli are typically  $\sim$ MPa. It will be shown that the stresses required to explain the thermal contraction are consistent with those observed in shrinkage experiments.

The large negative expansivities arise essentially because of the reduction in the moduli of the samples with increasing temperature. In high density polyethylene it is believed to be due to the reduced effectiveness of the crystalline bridges due to increasing shear lag associated with the  $\alpha$ -relaxation process. Our theory is, however, a general one and can be developed *ab initio* without such structural considerations. In this respect, it is therefore of wide possible application.

The strain,  $e$ , in a sample subjected to a stress,  $\sigma$ , depends on the sample modulus  $E$  and consequently the apparent thermal expansion coefficient  $\alpha$  depends on the temperature dependence of  $E$  and  $\sigma$ . Specifically:

$$\alpha = \frac{de}{dT} = \left( \frac{\partial e}{\partial E} \right)_{\sigma, T} \frac{dE}{dT} + \left( \frac{\partial e}{\partial \sigma} \right)_{TE} \frac{d\sigma}{dT} + \left( \frac{\partial e}{\partial T} \right)_{E, \sigma} \quad (4)$$

The partial differentials in the above equation may be re-written in terms of  $e, \sigma, E$  and  $\alpha_0$  the ‘intrinsic’ expansion coefficient of the structure:

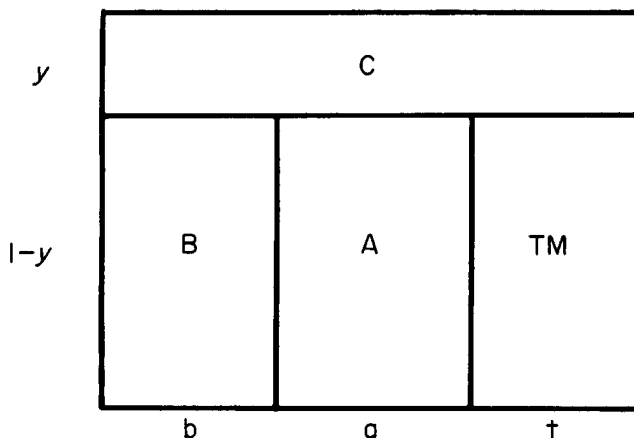
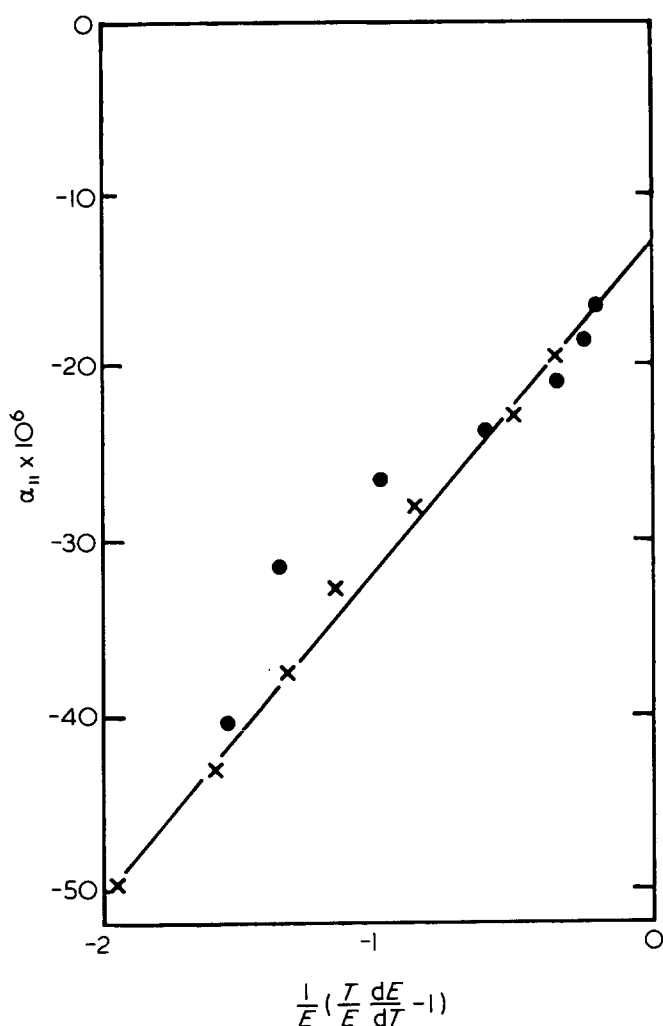


Figure 11 Schematic diagram of an oriented polymer considered to consist of a crystalline block (C), crystal bridges (B), amorphous material (A) and taut-tie molecules (TM)



**Figure 12** Variation of the thermal expansion coefficient of the low draw ratio film samples with the temperature/modulus function derived in equation (6). Crosses correspond to the 002-55 copolymer with  $\lambda=5.5$  and the dots to the 006-60 homopolymer with  $\lambda=6.5$

$$\alpha = -\frac{\sigma}{E^2} \frac{dE}{dT} + \frac{1}{E} \frac{d\sigma}{dT} + \alpha_0 \quad (5)$$

The temperature dependence of the modulus is an experimentally measured quantity, but we must make some assumption about the temperature dependence of  $\sigma$ . For simplicity we have taken  $\sigma$  to be given by an expression similar to that for ideal rubber elasticity i.e.  $\sigma = -BT$  where  $B$  depends upon parameters of the network. Numerical calculations based on figures derived from work by Ciferri, Hovee and Flory<sup>11</sup>, show that the alternative assumption  $\sigma = -(A + BT)$ , which is equivalent to introducing an internal energy term, has a negligible effect on the predicted thermal expansion coefficient although a different numerical value for  $B$  will be obtained. (Additionally, we ignore the small change in  $\sigma$  produced by thermal strains as we imagine the network strain to be very large compared with these strains). Hence we finally obtain:

$$\alpha - \alpha_0 = -\frac{B}{E} \left[ 1 - \frac{TdE}{EdT} \right] \quad (6)$$

For LPE the modulus decreases with temperature and hence the term in the brackets is positive thus giving  $\alpha$

values lower than  $\alpha_0$ . The nature of the contracting force has not been specified. There is a contribution from the measurement system but this is a small correction and has been ignored in the present argument. The main assumption is that the force is entropic and as a magnitude guideline we will consider the forces measured when samples are immersed at constant length in an oil bath. These shrinkage forces have been measured at various bath temperatures and correspond to stresses in the 10 to 30 MPa region over the sample cross-section.

The validity of equation (6) can be checked by measurements of the variation of the modulus with temperature of the samples used for the expansion measurements. The 10 second static modulus was selected for this purpose and observations were made for a number of film samples over a range of temperatures. If the expansion coefficients for various temperatures are plotted against the corresponding values of  $(1/E)[(T/E)(dE/dT) - 1]$ , equation (6) predicts a straight line with a slope  $B$  and an intercept on the  $\alpha$  axis of  $\alpha_0$ . We would expect the value of  $\alpha_0$  at the higher draw ratios to approach the  $c$ -axis crystalline value since above draw ratios of about 10 the structure is assumed to be microfibrillar with the crystalline regions, possibly with intercrystalline bridges, providing the dominant component in the draw direction. At low draw ratios the structure is less well defined and  $\alpha_0$  more difficult to anticipate. The results obtained for three draw ratios of each polymer are plotted in *Figures 12, 13 and 14* and apart from the low draw ratio 006-60 sample show a reasonably linear relationship. The values obtained for  $\alpha_0$  and  $B$  by fitting lines to the points are given in *Table 2*. The  $\alpha_0$  values fall within the expected area with little difference between the two polymers. The shrinkage stresses increase with draw ratio, ranging from 0.019 MPa per degree to 0.075 MPa per degree. Column 4 in *Table 2* shows the corresponding stresses which would be present at 76°C while column 5 shows the shrinkage stresses measured when similar samples are immersed in a silicone oil bath at this temperature. Again the agreement between the shrinkage force measurements and the values calculated from the  $B$  factors is fairly good in view of the variations found in the shrinkage measurements. The modulus variation contributes substantially to the observed expansion coefficient. As an example, the values obtained for  $(1/E)(dE/dT)$  at draw ratio 11 with 006-60 film vary between  $-1.9 \times 10^{-3} \text{ K}^{-1}$  at  $-40^\circ\text{C}$  (223 K) and  $-16 \times 10^{-3} \text{ K}^{-1}$  at  $20^\circ\text{C}$  (293 K).

The rod samples have not been examined in such detail but modulus measurements at various temperatures have been determined for the extruded polymers by a static three point bend test. The measurements of the expansion coefficients over the high and low temperature ranges can then be combined by selecting the centre point of each and, with the corresponding modulus values, calculating the values of  $\alpha_0$  and  $B$ . The values obtained are given in *Table 4* and show a gradual decrease in  $\alpha_0$  with draw ratio to values slightly above the film values while the shrinkage forces generally are at a lower level. Shrinkage force measurements on all the rods are not available but individual samples of deformation ratio 15:1 have given values of 6 MPa at  $100^\circ\text{C}$ .

Similar results on the die drawn 002-55 polymer are also shown in *Table 4*. These show stress levels close to those found with the extruded samples with  $\alpha_0$  values approaching the  $c$  axis crystal value.

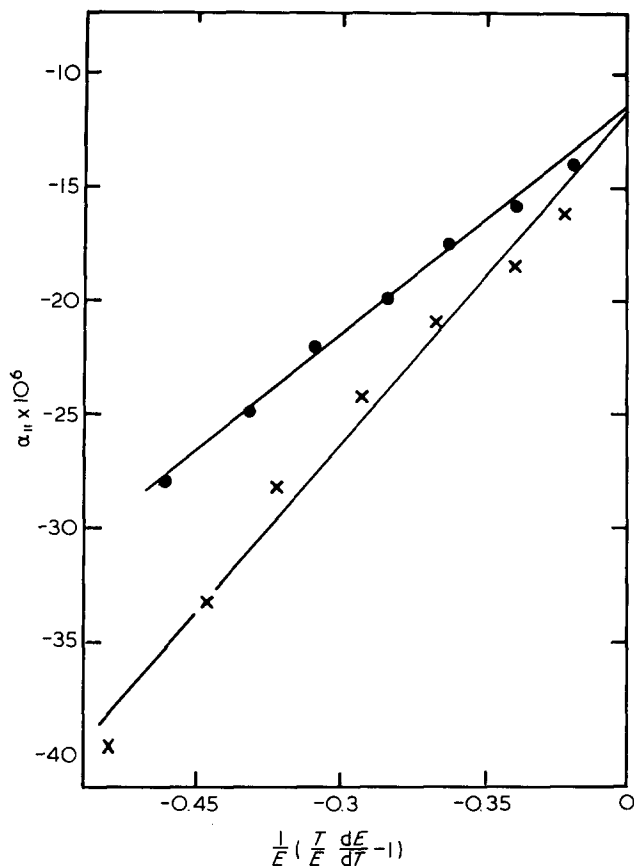


Figure 13 As Figure 12 but with draw ratios of 11 for both polymers

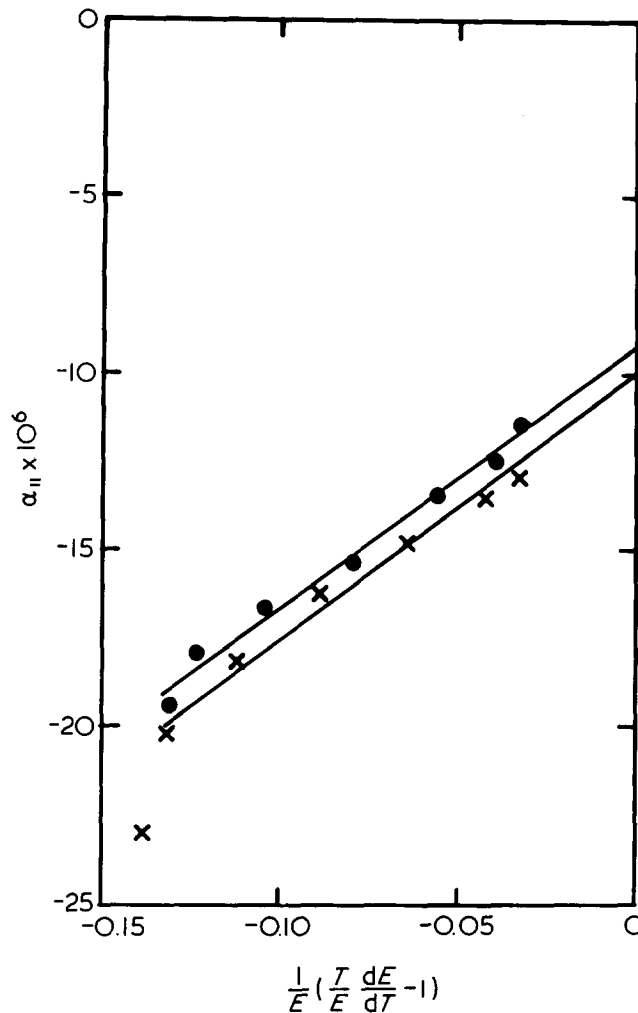


Figure 14 As Figure 12 but with draw ratios of 19 for the copolymer and 20 for the homopolymer

CONCLUSIONS

This analysis shows that the anomalous negative expansion coefficients measured in highly oriented polyethylene samples are not simply due to the negative expansion coefficient of the crystalline regions but can be attributed to an internal stress in the sample which causes a changing strain as the sample modulus, and to a lesser extent, the internal stress, vary with temperature.

The wide divergence between the rod and film measurements can be explained on the basis of different residual shrinkage stresses introduced into the polymers during processing. The intrinsic or strain free axial expansion coefficients ( $\alpha_0$ ) appear to decrease less rapidly with draw ratio for the rods than for the films but within experimental error the final levels reached do not exceed the *c*-axis crystal expansion level of  $-12 \times 10^{-6} \text{ K}^{-1}$ .

ACKNOWLEDGEMENTS

Thanks are due to Mr J. Defty for his careful measurements of the film shrinkage forces.

The thermal expansion instrumental development was initiated by Dr A. G. Gibson, further developed in cooperation with Dr M. J. Booth and patiently constructed by Mr D. Armitage. Thanks are also due to Dr Booth for his contribution to the ensuing interpretation of the results obtained.

REFERENCES

1 Choy, C. L. 'Developments in Oriented Polymer (Ed I. M. Ward) Applied Science Publishers, London, Ch. 4 (1982)  
 2 Mead, W. T., Desper, C. R. and Porter, R. S. *J. Polym. Sci., Polym. Phys. Edn.* 1979, 17, 859

Table 4 Values derived from the rod measurements for the stress constant *B* and the intrinsic expansion coefficient  $\alpha_0$  in equation (6) with calculated internal stresses at the processing temperature

Polymer	Deformation ratio	$\alpha_0 \times 10^6$	<i>B</i> (MPa/°C)	Stress at 100°C (MPa)
<i>Extruded rod</i>				
R006-60	5.1	-4.6	0.008	3.0
	10.0	-7.6	0.012	4.5
	14.8	-8.7	0.026	9.7
	20.0	-7.7	0.064	24
R40	4.9	1.4	0.003	1.1
	9.9	-5.3	0.009	3.4
	15.0	-8.2	0.039	15
	19.5	-9.1	0.059	22
<i>Die drawn rod</i>				
R002-55	Draw ratio			
	5.8	-6.0	0.019	7.1
	10.2	-11.9	0.016	6.0
	10.7	-10.5	0.020	7.5

3 Gibson, A. G. and Ward, I. M. *J. Mater. Sci.* 1979, 14, 1838  
 4 Choy, C. L., Chen, F. C. and Young, K. *J. Polym. Sci., Polym. Phys. Edn.*, 1981, 19, 335  
 5 Gibson, A. G. and Ward, I. M. *J. Polym. Sci., Polym. Phys. Edn.* 1979, 16, 2015  
 6 Hope, P. S., Gibson, A. G. and Ward, I. M. *J. Polym. Sci., Polym. Phys. Edn.* 1980, 18, 1243  
 7 Gibson, A. G. and Ward, I. M. *J. Mater. Sci.* 1980, 15, 979  
 8 Brew, B., Hope, P. S. and Ward, I. M., to be published  
 9 Capaccio, G. and Ward, I. M. *Colloid Polym. Sci.* 1982, 260, 46  
 10 Struick, L. C. E. *Polym. Eng. Sci.* 1978, 18, 799  
 11 Ciferri, A., Hoeve, C. A. and Flory, P. J. *J. Am. Chem. Soc.* 1961, 83, 1015